High-beta physics of magnetic islands in 3-D equilibria

C. C. Hegna[1], M. G. Schlutt[1], E. D. Held[2],
S. E. Kruger[3] and C. R. Sovinec[1]
[1]University of Wisconsin, Madison, WI, 53705
[2]Utah State University, Logan, UT
[3]Tech-X Corporation, Boulder, CO

Abstract
Numerical simulation and analytic theory are used to describe the effects of finite plasma pressure on magnetic island formation and magnetic surface fragility in three-dimensional geometry. The extended MHD code NIMROD is used to simulate high-beta physics in net current-free straight stellarator geometry using a resistive MHD model with anisotropic heat conduction. A connection between 3-D geometry, flux surface destruction and the breaching of MHD stability boundaries is investigated. Analytic calculations of magnetic island formation in 3-D equilibria employ drift kinetic theory to describe self-consistent current responses. Three dimensional components of $1/B^2$ produce net radial drifts that give rise to viscous forces on the plasma and reactive responses to the 3-D fields that describes in-surface currents. Generally, the reactive in-surface currents counteract the island producing effects due to resonant Pfirsch-Schlüter currents.

I. Introduction

The theory of 3-D MHD equilibria is one of the oldest problems in magnetic confinement theory. Unlike axisymmetric equilibria, where the existence of robust topologicially toroidal magnetic surfaces are guaranteed to exist, 3-D equilibria generally contain magnetic islands and regions of magnetic stochasticity. As such, a complete description of 3-D equilibria requires an understanding of the physics that influences magnetic island formation, island overlap and magnetic stochasticity. The theory of nonlinear magnetic island growth and saturation is conventionally described as the nonlinear consequence of tearing mode instabilities. In this sense, the lack of a continuous symmetry blurs the difference between conventional tokamak notions of equilibrium and non-ideal MHD stability. Indeed, analytic efforts to describe saturated magnetic island widths in 3-D equilibria using a resistive MHD model show a dependency of the saturated island widths on resistive MHD 'stability' parameters [1]. In high temperature plasmas, magnetic island physics is highly sophisticated and involves a number of effects beyond those described by MHD theory.

Numerical simulation and analytic theory are used to describe the effects of finite plasma pressure on magnetic island formation and magnetic surface fragility in three-dimensional geometry. The extended MHD code NIMROD [2] is used to investigate high-β properties of net current-free straight stellarator geometry using a resistive MHD model with anisotropic heat conduction. This approach to describing high-β stellarator behavior is distinctly different than conventional approaches used to construct solutions to the 3-D MHD equilibrium equations that rely on simplifications in the physics describing magnetic surface breakup [3]. For the calculations reported here, the effects of breaching instability boundaries in 3-D configurations and their nonlinear consequences are monitored in the simulations.

In an effort to describe physics beyond the MHD model, analytic calculations of magnetic island formation in 3-D equilibria employ drift kinetic theory to describe self-consistent current responses. In response to 3-D variations in field strength, a kinetic distortion develops that has both a reactive and a dissipative response. While the dissipative response is used to describe viscous torques and their corresponding effect on neoclassical transport, the reactive response describes currents flowing within the magnetic surfaces that are stabilizing to magnetic island formation in 3-D configurations.

II. Resistive MHD simulations of 3-D configurations

In this work, numerical simulations of straight stellarators are performed with the NIMROD code. The MHD equations are advanced in time, yielding a description of the evolution of a 3-D configuration that starts from vacuum magnetic fields and progresses through the formation of stable equilibria at low β via a heating source. Further heating violates MHD instability boundaries at higher β and finally the discharge terminates due to pressure-induced magnetic stochasticity.

A 3-D vacuum magnetic field with finite rotational transform is initialized. Finite-β equilibria are generated by introducing a heating source into the plasma domain and evolving the full resistive MHD equations in time. The simulations employ anisotropic heat conduction with typical ratios of parallel to perpendicular heat diffusivities $\chi_{||}/\chi_{\perp} \sim 10^5 - 10^8$. The initial vacuum solution can be specified to have a helical symmetry or to be spoiled by the introduction of small 3-D components. With finite parallel heat conduction, pressure gradients are allowed to persist in regions with small magnetic islands or magnetic stochasticity as has been implied in recent stellarator experiments [4].

For all the simulations presented here, the initial vacuum magnetic field has a dominant $m/n = 2/2$ vacuum harmonic that produces helically rotating oblate magnetic surfaces. The rotational transform profile is monotonically increasing with stellarator-like magnetic shear, $\iota(0) \approx 0.4, \iota_a \approx 1$. Characteristic parameters of these plasmas are $\mathbf{B}_z = 1T, L = 2\pi m, a_{eff} = 0.2m, \beta_{max} = 2\mu_o < p > /B_z^2 \sim 3 - 5\%, S = \tau_R/\tau_A = 1 - 4 \times 10^5, \tau_E = a^2/4\chi_{\perp} = 0.01s$. Early in the simulation, robust magnetic surfaces are observed.

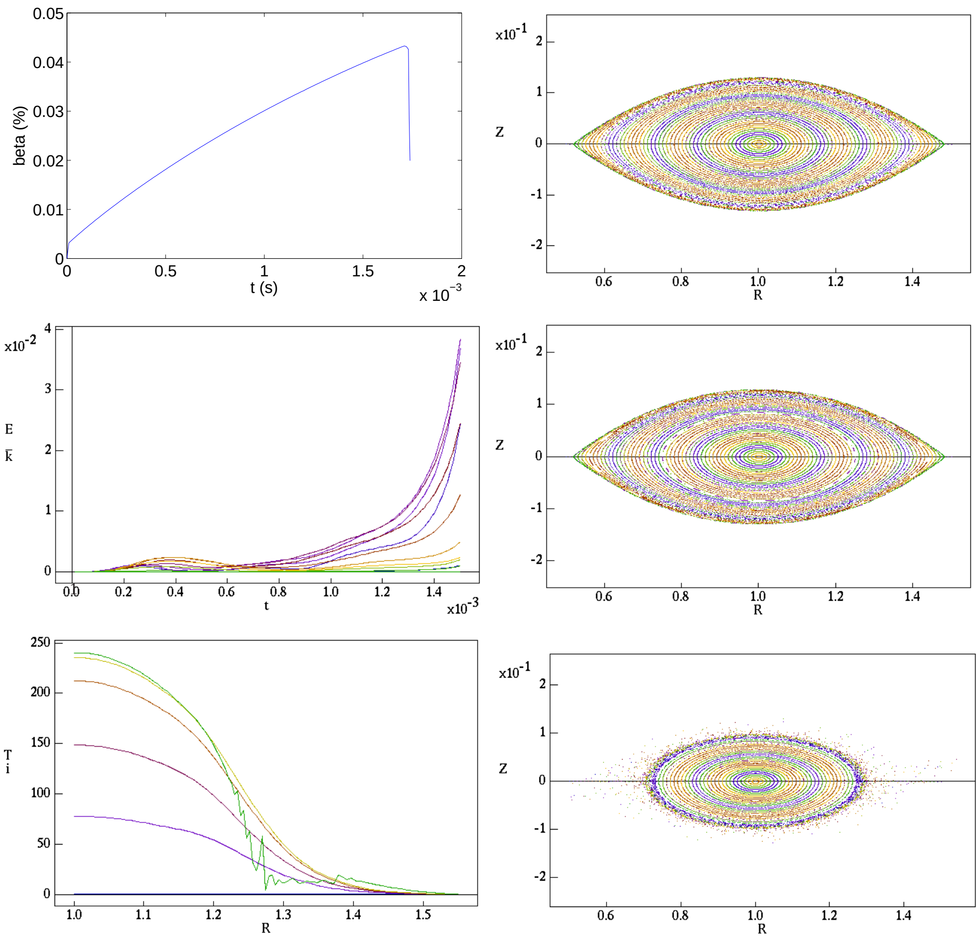

Figure 1 - The evolution of β, kinetic energy perturbations, temperature profiles at various times and Poincare plots of the magnetic field at $t = 0, t = 1.0 \times 10^{-3}$ and $t = 1.73 \times 10^{-3}$. For this case, only even n harmonics are allowed in the simulation (i. e., only stellarator symmetric perturbations are present).

The case shown in Figure 1 corresponds to a configuration initialized with a perfectly helically symmetric vacuum magnetic field. Since a continuous symmetry is present in this configuration, Grad-Shafranov equilibria can be generated if no instability boundaries are breached. Plasmas heating produces finite β plasmas with good magnetic surfaces early in time. At $\beta \sim 3\%$, MHD perturbations with a dominant $n = 2$ harmonic are excited and grow with continued heating. As β increases, the degree of stochasticity in the edge region grows. At late times, the temperature profile collapses as shown in the figure in the lower left and the β value abruptly drops from its peak value $\beta \sim 4.5\%$ to zero. For this case, the dominant mechanism for the β collapse is the degradation of the magnetic surface quality. Magnetic stochasticity grows from the edge region toward the core as β increases.

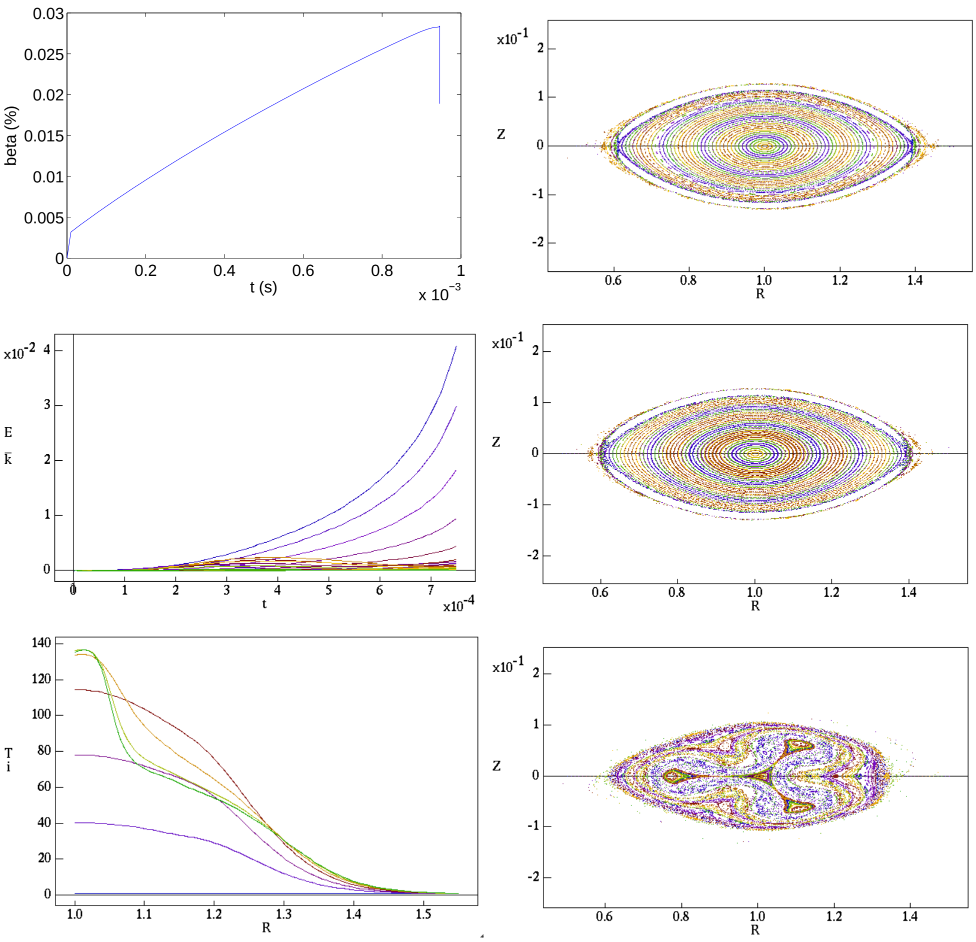

Figure 2- The evolution of β, kinetic energy perturbations, temperature profiles at various times and Poincare plots of the magnetic field at $t = 0, t = 4.8 \times 10^{-4}$ and $t = 9.2 \times 10^{-4}$. The initial vacuum magnetic field has a continuous symmetry. Stability of the helically symmetric equilibrium by introducing small symmetry breaking perturbations into the system.

As in the case shown in Figure 1, the initial configuration for the case shown Figure 2 is helically symmetric. However, in this simulation, small $n = 1$ symmetry breaking perturbations are excited to probe the stability of odd-n harmonics. At early times, these harmonics do not grow and the equilibrium remains perfectly helically symmetric. However, at $\beta \sim 1\%$, an instability with a dominant $n = 1$ structure grows in time. With the presence of an $\iota\!\!\!- = 0.5$ surface in the core, prominent $n = 1$ structures appear that enhances the degree of stochasticity in the system relative to the case shown in Figure 1. As in the first case, the temperature profile collapses due to the prevalence of magnetic stochasticity late in the simulation with a peak $\beta \sim 2.8\%$ that is considerably lower than that obtained in the first simulation.

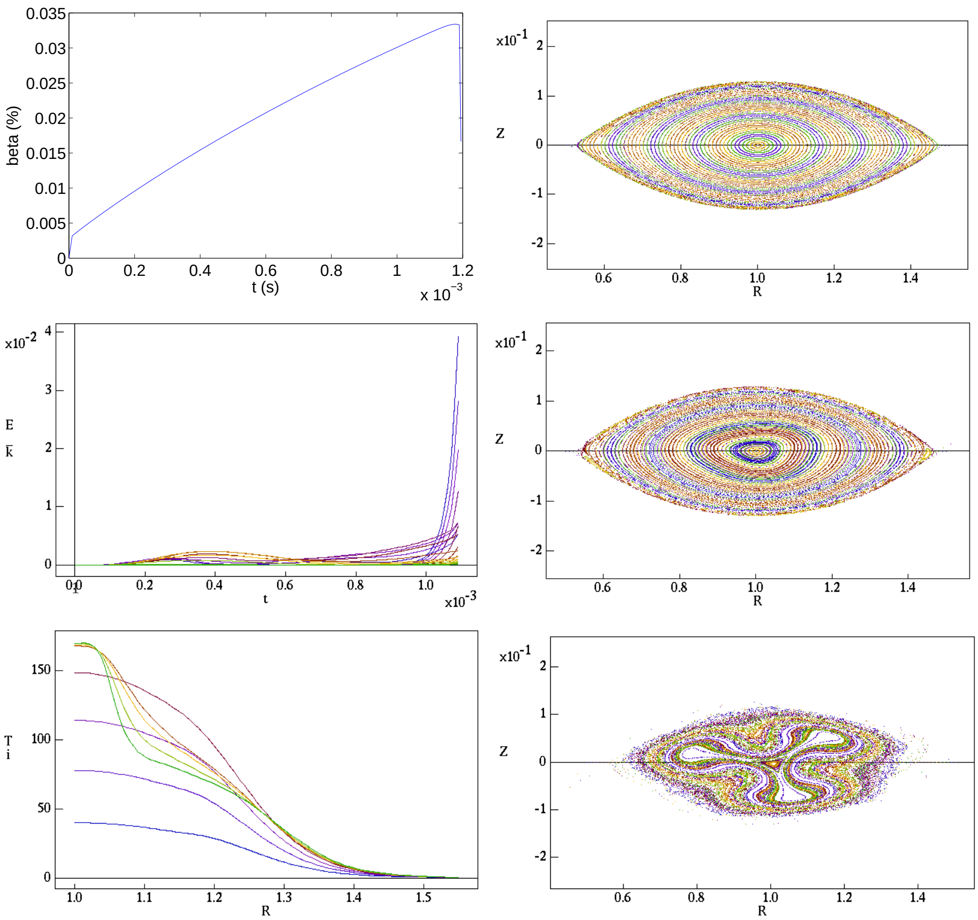

Figure 3- The evolution of β, kinetic energy perturbations, temperature profiles at various times and Poincare plots of the magnetic field at $t = 0, t = 1.0 \times 10^{-3}$ and $t = 1.18 \times 10^{-3}$. Unlike the cases shown in Figs. (1) and (2), the vacuum solution contains small levels of 3-D magnetic field perturbations.

The distinguishing property of the case shown in Figure 3 relative to the first two cases is the presence of 3-D components in the vacuum configuration. A collection of small $\sim 10^{-4}$ magnetic harmonics of incommensurate helicity are present from $t = 0$ in the simulation. Subsequent finite-β equilibria are 3-D. As shown in the middle figure on the left, the presence of the 3-D vacuum components delay the onset of MHD instabilities with dominant $n = 1$ harmonics until $\beta \sim 3\%$ is reached. While the profiles and the gross macroscopic features are largely the same between the simulations shown in Figs. (2) and (3), the onset condition for MHD instability and the peak β are notably different. This suggest that the presence of intrinsically 3-D magnetic field configurations can be a benefit to the stability properties.

The numerical experiments shown in Figures (1)-(3) can be repeated for configurations without an $\iota = 0.5$ rational surface present in the configuration. While there are detailed differences, the trend is the same. We have found cases where the plasma tends to be more resilient to instability and have higher peak β values when 3-D components are present in the vacuum magnetic field configuration.

III. Kinetic shielding of magnetic islands in 3-D equilibria

While MHD based models provide a useful basis for studying high-β properties of 3-D configurations, kinetic physics can also influence magnetic island physics in 3-D configurations. In this section, a kinetic theory for 3-D plasmas is developed to describe non-MHD physics modifications to isolated magnetic island formation.

In general 3-D equilibria, singular currents arise at rational surfaces if topologically toroidal magnetic flux surfaces are assumed [1]. If flux surfaces ψ exist, the equilibrium magnetic field can be written $\mathbf{B} = q\nabla\psi \times \nabla\theta + \nabla\zeta \times \nabla\psi$ and the equilibrium current profile can be written $\mathbf{B} = \lambda\mathbf{B} + \mathbf{B} \times \nabla p/B^2$. Writing the parallel current $\mathbf{J} \cdot \mathbf{B}/B^2 = \lambda$ and $1/B^2$ in Fourier series, $\lambda = \Sigma_{mn}\lambda_{mn}e^{im\theta - n\zeta}, 1/B^2 = B_{00}^{-2}[1 + \Sigma_{mn}\delta_{mn}e^{im\theta - in\zeta}]$, the quasineutality condition $\nabla \cdot \mathbf{J} = 0$ is $\Sigma_{mn}e^{im\theta - in\zeta}[(m - nq)\lambda_{mn} + (dp/d\psi)\delta_{mn}(mG + nI)/B_{00}^2] = 0$. Solutions to this equation have contributions of the form $\lambda_{mn} \sim p'\delta_{mn}(m - nq)^{-1}$. Resonant components of the Pfirsch-Schlüter current solution have "$1/x$"-like singularities at the rational surfaces $q = m/n$ when $\delta_{mn} \neq 0$. This singularity can be resolved by allowing for magnetic islands at the rational surface. Self-consistent solutions for the magnetic island width find that the island resolved Pfirsch-Schlüter currents provide a mechanism to support the existence of this island.

In addition to Pfirsch-Schlüter currents, non-ideal MHD effects can also produce resonant responses. In 3-D plasmas, variations of the viscous contribution to the momentum balance produces perpendicular currents that vary within the magnetic surface. Including this contribution to quasineutrality $[S = \sqrt{g}\nabla \cdot \mathbf{J}_{\perp,\nu} = \sqrt{g}\Sigma_s\nabla \cdot (\mathbf{B} \times \nabla \cdot \vec{\vec{\pi}}_s/B^2) = \Sigma_{mn}iS_{mn\nu}e^{im\theta - in\zeta}]$ produces an additional source in the general solution for λ_{mn}

$$\lambda_{mn} = \frac{S_{mn\nu}}{m - nq} - \frac{dp}{d\psi}\frac{mG + nI}{B_{00}^2}\frac{\delta_{mn}}{m - nq} + \Delta'_{mn}A_{mn}\delta(\psi - \psi_{mn}). \quad (1)$$

The Pfirsch-Schlüter current and the first term due to the viscous source have the $1/(m - nq)$ singular structure. The third term is a homogeneous solution to the quasineutrality equation for the resonant harmonic of the parallel current.

In order to resolve the singular response at $q(\psi_o) = m/n$, the presence of a magnetic island chain is assumed. Its presence is incorporated into deriving self-consistent island localized plasma currents due to both MHD and kinetic responses. Ampere's law is then used to derive self-consistent magnetic island widths. The magnetic field is now described by $\mathbf{B} = \nabla\alpha \times \nabla\psi + \nabla\Psi^* \times \nabla\chi$ where ψ serves as a radial-like variable, $\alpha = m\theta - n\zeta$ is the helical angle of the island and χ is a poloidal angle like variable. The magnetic field lines lie on surfaces of constant $\Psi^* = q'_o x^2/2 - A\cos(n_o\alpha)$ where $q'_o = dq/d\psi|_{\psi=\psi_o}$, $x = \psi - \psi_o$ and A is the island producing magnetic field. The island width is given by $w = 4\sqrt{|A/q'_o|}$

An analytic theory is developed to describe kinetic modifications to magnetic island width predictions of 3-D equilibria [5]. Drift kinetic theory is used to calculate non-resistive MHD corrections to conventional analytic island theory [1] for a quasi-symmetric configuration with $B = B_o[1 - \epsilon_h\cos(M\theta - N\zeta) + \delta B(\psi,\theta,\zeta)$ where $M\theta - N\zeta$ denotes the dominant helical angle and the 3-D sidebands are assumed small ($\delta B \ll \epsilon_h$). A kinetic theory is used to deduce the effect of the helical side bands on trapped particles in collisionless regimes. The bounce averaged kinetic equation is given by

$$< \frac{\partial f^1}{\partial t} > + < \mathbf{v}_E\cdot\nabla\alpha + \mathbf{v}_d^0\cdot\nabla\alpha > \frac{\partial f^1}{\partial\alpha} - < C(f^1) > = - < \mathbf{v}_d^1\cdot\nabla\Psi^* > \frac{\partial f_M}{\partial\Psi^*}, \tag{2}$$

where the source term on the right denotes net radial drift of the trapped particles off the magnetic surfaces due to 3-D components of $1/B^2$ and the terms on the left describes the contribution from $\mathbf{E}\times\mathbf{B}$ and precessional drifts within the flux surface and collisions. This kinetic distortion is conventionally used to construct neoclassical transport in high temperature stellarators or equivalently the neoclassical toroidal viscosity (NTV) of tokamak theory when axisymmetry is perturbed by small 3-D fields [6]. However, in addition to this dissipative response, the kinetic distortion also describes a reactive response that influences magnetic island physics. Solutions to this equation are included in the quasineutrality equation

$$\mathbf{B}\cdot\nabla\lambda + \Sigma_s q_s \int d^3\mathbf{v}(\mathbf{v}_d^1\cdot\nabla f_M + \mathbf{v}_d^0\cdot\nabla f^1) = 0, \tag{3}$$

where superscripts 0(1) on the magnetic drift terms ($\mathbf{v}_d$) are calculated using the quasi-symmetric (3-D) components of the magnetic field strength. In the zero island width limit, the solution to Eq. (3) is given by Eq. (1) where the middle term in the above describes the MHD physics source for the Pfirsch-Schlüter current and the last term produces the viscous source.

Using Eq. (3) to solve for the island resolved parallel current and Ampere's law, a self-consistent expression for the magnetic island width can be derived. In the absence of the kinetic response, the saturated island width given by $|q'_o w| \approx \sqrt{C\delta_{mn}}$, where $C \sim \beta_\theta$ and δ_{mn} is the strength of the 3-D component of the magnetic field.

In general, the kinetic response has both 'reactive' and dissipative contributions. The dissipative response is used to calculate the net viscous force on the plasma that affects toroidal flow profile evolution [7]. The reactive response describes currents that flow within the magnetic surface producing magnetic fields in-phase with the island producing magnetic field. Generally, the reactive response is largest at smallest collisionality. Two classes of 3-D magnetic fields can produce net radial particle drifts. The first is the $\mathcal{O}(\delta)$ contributions to the magnetic field spectrum. Of particular importance is that part of f^1 driven by the resonant component of $1/B^2 \sim \delta_{mn}$. The second contribution is due to the island's self-consistent deformation of the magnetic field spectrum as originally pointed out by Shaing [8].

Recalculating the self-consistent island width accounting for the kinetic modifications leads to a prediction for the saturated island width of the form

$$|q_o' w|^2 \approx C\delta_{mn}(1-\mathcal{R})(1-\frac{w}{w_c}), \tag{4}$$

where $w_c \sim \delta_{mn}(1-\mathcal{R})/\epsilon_h' \mathcal{R}_w$. Here $\mathcal{R}$ and $\mathcal{R}_w$ characterize the strength of the kinetic responses. The expressions for these two quantities are kinetic space integrals over trapped particle space with characteristic amplitude $\mathcal{R} \sim \mathcal{R}_w \sim \sqrt{\epsilon_h}$ in the zero collision frequency limit. With small kinetic shielding, the saturated island width scales as $\delta_{mn}^{1/2}$. With kinetic responses, the saturated island width effectively scales as $w \sim w_c \sim \delta_{mn}$. Since $\delta_{mn} \ll 1$, the kinetic effects substantially reduce the predicted island width.

The implication of this work is that at high temperature, kinetic corrections to magnetic island physics are significant in 3-D configurations. High temperature stellarators are more resilient to flux surface breakup than theoretical predictions using conventional MHD models would imply. In order to calculate the kinetic responses, closure calculations would need to be coupled to extended MHD numerical tools. In particular, to account for the effects discussed here, drift kinetic theory would be required to calculate the pressure anisotropy and the associated contributions to the fluid momentum balance through the closure contribution $\nabla \cdot \vec{\vec{\pi}}_s$.

Acknowledgments

This work is supported by the U. S. Department of Energy through the grants DE-FG02-86ER53218 and DE-FG02-99ER54546.

References

[1] J. R. Cary and M. Kotscheneuther, Phys. Fluids **28**, 1392 (1985); C. C. Hegna and A. Bhattacharjee, Phys. Fluids B **1**, 392 (1989); A. Bhattacharjee et al, Phy. Plasmas **2**, 883 (1995).

[2] C. R. Sovinec et al, J. Comp. Phys. **195**, 355 (2004).

[3] S. P. Hirshman et al, Comput. Phys. Commun. **43** 143 (1986); A. H. Reiman and H. S. Greenside, Comput. Phys. Commun. **43** 157 (1986); K. Harakuji et al, J. Comput. Phys/ **81** 169 (1989).

[4] A. Reiman et al, Nucl Fusion **47**, 572 (2007).

[5] C. C. Hegna, submitted to Plasma Physics and Controlled Fusion (2010).

[6] K. C. Shaing, Phys. Plasmas **10**, 1443 (2003).

[7] J. D. Callen et al, Nucl. Fusion **49**, 085021 (2009); J. D. Callen et al, Phys. Plasmas **16**, 082504 (2009).

[8] K. C. Shaing, Phys. Rev. Lett. **87**, 245003 (2001).